Optimum vegetation characteristics, assimilation, and transpiration during a dry season: 1. Model descripton

van der Tol, C.; Meesters, A.G.C.A.; Dolman, A.J.; Waterloo, M.J.

published in
Water Resources Research
2008

DOI (link to publisher)
10.1029/2007WR006241

document version
Publisher's PDF, also known as Version of record

WATER RESOURCES RESEARCH, VOL. 44, W03421, doi:10.1029/2007WR006241, 2008

Optimum vegetation characteristics, assimilation, and transpiration during a dry season: 1. Model description

C. van der Tol,[1,2] A. G. C. A. Meesters,[1] A. J. Dolman,[1] and M. J. Waterloo[1]

Received 8 June 2007; revised 3 December 2007; accepted 12 December 2007; published 21 March 2008.

[1] This paper presents a model to predict optimum vegetation characteristics in water stressed conditions. Starting point is the principle of homeostasis of water flow through the soil-vegetation-atmosphere continuum. Combining this with a biochemical model for photosynthesis, a relationship between photosynthetic capacity, stomatal regulation, and hydraulic properties of the vegetation is derived. Optimum photosynthetic capacity and internal carbon dioxide concentration are calculated using the assumption that growth is maximized. This optimality hypothesis is applied for three scenarios which are increasingly realistic. Optimum parameters reflect a strategy to deal with two tradeoffs: the trade-off between fast growth and avoidance of drought and between a high photosynthetic capacity and avoidance of high respiration losses. The theory predicts general boundary conditions for growth but does not consider effects of competition between species, fires, pest, and diseases or other limitations that occur locally. In a companion paper the theory is evaluated using a data set collected in sub-Mediterranean vegetation.

Citation: van der Tol, C., A. G. C. A. Meesters, A. J. Dolman, and M. J. Waterloo (2008), Optimum vegetation characteristics, assimilation, and transpiration during a dry season: 1. Model description, *Water Resour. Res.*, *44*, W03421, doi:10.1029/2007WR006241.

1. Introduction

[2] Most climate models today calculate photosynthesis and the carbon balance beside the water and energy balance [*Sellers et al.*, 1997]. The current interest of climatologists in photosynthesis has two reasons. First, the insight has grown that carbon dioxide plays an important role in the climate system [*Schimel*, 1995], and second, studies of the physiology of plants have led to the understanding that the processes of photosynthesis and transpiration are so closely connected that the fluxes of water and energy can really only be understood by also describing photosynthesis [*Jones*, 1998].

[3] The biochemical processes involved in photosynthesis, transpiration and growth at organelle to canopy scale are now reasonably well understood, at least at the level of detail relevant for climate modelers (among others, *Tuzet et al.* [2003]). Coupling of the biochemical and surface exchange processes in physically based models makes it possible to predict changes of the Earth surface cover as a result of climate change, or, conversely, changes in climate as a result of surface cover changes [*Kabat et al.*, 2004].

[4] Despite the increased process knowledge, two important almost classic questions concerning spatial modelling of surface exchange processes have remained: how to apply process understanding at the desired spatial and temporal scale and how to attribute values to the biochemical parameters of the surface that are highly variable both in space and time [*Baldocchi et al.*, 2002].

[5] An approach to deal with these questions has been to order the vegetation on earth into so called plant functional types (PFTs). The concept is attractive and has been applied in large models, which successfully reproduced spatial patterns of ecosystems [*Smith et al.*, 1997; *Kucharik et al.*, 2000]. A limitation of such models is that parameters of functional types have fixed, a priori values. The concept is therefore not suitable to explain why PFTs exist and how the differences among them have evolved.

[6] This paper addresses the question of parameter estimation. A method is presented to predict biochemical parameters from climatic constraints only. This enables us to say something about ranges of credible parameter values in a specific climate. Approaches to predict biochemical parameters from climatic constraints which have been developed earlier are used as a starting point.

[7] One approach to predict biochemical parameters is to use the principle of homeostasis of water flow through the soil-vegetation-atmosphere continuum. From the idea that xylem embolism must be avoided, allocation between root and shoot can be derived [*Magnani et al.*, 2000; *Sperry et al.*, 2002; *Mencuccini*, 2003]. Using the same principle, *Katul et al.* [2003] derived a relationship between photosynthetic capacity and hydraulic properties of the vegetation. This relationship is also used in this study.

[8] Another approach to predict biochemical parameters is to consider trade-offs in terms of cost and benefit [*Smith and Huston*, 1989]. *Rodriguez-Iturbe et al.* [2001] evaluated two coexisting strategies: shallow-rooted vegetation which

[1]Department of Hydrology and Geo-Environmental Sciences, Vrije Universiteit Amsterdam, Amsterdam, Netherlands.
[2]Now at ITC International Institute for Geo-Information Science and Earth Observation, Enschede, Netherlands.

0043-1397/08/2007WR006241$09.00

Table 1. Most Important Variables and Parameters Used in the Model

Parameter	Definition	Unit of Measure
C_a	atmospheric carbon dioxide concentration	mol m^{-3}
C_i	intercellular carbon dioxide concentration	mol m^{-3}
D	vapour pressure deficit	mol m^{-3}
E	transpiration rate	mol m^{-2} s^{-1} or mm d^{-1}
g	effective surface conductance (stomatal aerodynamic)	m s^{-1}
G	growth (net photosynthesis less maintenance respiration)	mol m^{-2} s^{-2}
m_d	daytime maintenance respiration coefficient	
m_n	nighttime maintenance respiration coefficient	
Q	growth integrated over the season	mol m^{-2}
r	ratio of assimilation to nonrecycled respiration	
R_{dd}	daytime dark respiration	mol m^{-2} s^{-1}
R_{dn}	nighttime dark respiration	mol m^{-2} s^{-1}
t	time	s or d
t_f	time at which water stress starts	s or d
t_e	length of the dry season	s or d
s_0	amount of water in root zone at $t = 0$	mol m^{-2} or mm
s_f	amount of water in root zone below which water stress occurs	mol m^{-2} or mm
s_r	amount of water in the root zone at wilting point	mol m^{-2} or mm
α	empirical, species	soil dependent drought response coefficient
γ	shape factor in the photosynthesis model	mol m^{-3}
Γ^*	carbon dioxide compensation point for photorespiration	mol m^{-3}
ε	coefficient for the effect of light-limited leaves in the canopy	
ν	photosynthetic capacity	mol m^{-2} s^{-1}
ξ	stress response function	

transpires intermittent rain quickly versus deep-rooted vegetation with a more steady transpiration rate. Later, *Laio et al.* [2001] modelled the water balance and soil moisture content as a function of a Poisson distributed rainfall, soil, and vegetation characteristics. *Daly et al.* [2004a, 2004b] used a similar concept to model growth as a function of intermittent precipitation. In their model, an expression for the integrated water stress over the growing season is used. Photosynthetic capacity is still a fixed parameter.

[9] In this paper, we study whether we can estimate biochemical parameters for dry conditions, in which a limited amount of water is available for transpiration. The hypothesis is used that this limited amount of water is used in such a way that net photosynthesis of the canopy is maximized.

[10] Two biochemical parameters are predicted: photosynthetic capacity and internal carbon dioxide concentration. We will argue that the values of these two parameters represent a strategy. The value of photosynthetic capacity can be seen as the result of a trade-off between a high rate of photosynthesis (high photosynthetic capacity) and a low risk of water stress (low photosynthetic capacity). The value of internal carbon dioxide concentration can be seen as reflecting a strategy to minimize photorespiration.

[11] First, a general model is presented which includes transport of water from the soil via the vegetation to the air, transport of carbon dioxide from air to mesophyll, and photosynthesis (section 2). Next, photosynthetic capacity, internal carbon dioxide concentration, and the seasonal cycle of photosynthesis and transpiration are calculated using the hypothesis that net photosynthesis during a growing season is maximized (from now on referred to as "optimality hypothesis"). This idea is applied to three scenarios, with increasing level of realism. In the first scenario (section 3) both environmental conditions and vegetation characteristics are constants. Maximum net photosynthesis and the biochemical properties are calculated for a prescribed, constant transpiration rate and constant humidity. In the second scenario (section 4), soil moisture content is modelled as a function of time. The vegetation interacts with a soil water reservoir which is not recharged. For a prescribed length of a dry period and initial soil moisture content, the seasonal cycle of transpiration and photosynthesis for which growth is maximized are calculated. In the third scenario (section 5), the initial size of the soil water reservoir is a stochastic variable. We will demonstrate that maximum growth is then reached when moderate water stress is tolerated but severe stress avoided.

[12] This paper focuses on how a canopy can most effectively transpire available water during a growing season in order to reach the highest rates of net photosynthesis. In an earlier study this approach resulted in a realistic evolution of stomatal regulation during a dry period [*Makela et al.*, 1996]. We now extend the approach to also model photosynthetic capacity.

[13] The model cannot explain other vegetation structure parameters because of three main limitations. First, it focuses on transpiration and uses the amount of water available for transpiration as input. Soil evaporation, evaporation of intercepted water, drainage, and surface runoff are not considered. Second, in the study the canopy is defined as the joint effect of all leaves together. The theory is not a classic ecological approach, since we do not use individuals as primary units and we do not model competition. The optimality hypothesis is applied to the level of a canopy. It is a physiological optimality hypothesis rather than an ecological optimality hypothesis. Third, the hypothesis of maximum growth has been disputed [*Kerkhoff et al.*, 2004]. Other hypothesis, such as avoidance of drought stress, may be equally valid. In this paper, drought stress is taken into account insofar as drought stress causes stomatal closure and negative net growth. Direct effects of drought stress such as wilting, heating of the canopy and salt stress are not

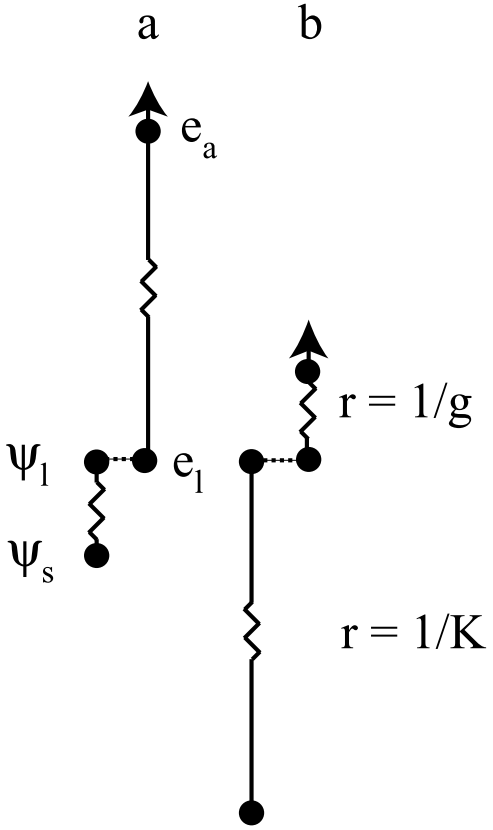

Figure 1. Schematic representation of gravity corrected water potentials in soil (ψ_s) and leaves (ψ_l) and partial vapor pressure in leaves (e_i) and air (e_a) and corresponding resistances r_h and r_s and conductances g and K for two different environmental conditions. Constant ψ_l is assumed. Potentials decrease towards the top of the figure. In scenario a, soil water potential and atmospheric vapor pressure are low (dry conditions). Hydraulic resistance has to be low compared to stomatal resistance. In scenario b, soil water potential and atmospheric vapor pressure are high (wet, humid conditions). Hydraulic resistance has to be high compared to stomatal resistance.

modeled explicitly. In a companion paper [*van der Tol et al.*, 2008] the theory is evaluated using field measurements in a sub-Mediterranean climate.

2. Coupling Carbon and Water Transport

[14] In this section, the principle of homeostasis of water transport through soil, vegetation, and atmosphere is combined with a photosynthesis model to derive the relation between biochemical parameters and environmental boundary conditions.

[15] Water flows from a relatively high water potential in the soil through the plant to a relatively low water potential in the leaf [*Dixon and Joly*, 1894; *Huber*, 1928]. The water potential in the leaf is in equilibrium with the partial vapor pressure in the stomata, which is generally higher than the partial vapor pressure in the ambient air. Consequently, water vapor is lost by diffusion to the air. Carbon dioxide diffuses from a relatively high partial pressure in the air to a relatively low partial pressure in the mesophyll. Both water flow and gas diffusion in the soil-plant-atmosphere system, although they are different processes, are usually described in analogy to Ohm's law:

$$F = g\Delta\psi \tag{1}$$

where F is a flux, g is a conductance, and $\Delta\psi$ is a potential gradient for the liquid phase and a concentration gradient for the vapor phase. Potentials are expressed on a volume base and have units of Pa, concentrations have units of mol m^{-3}. Fluxes are in mol m^{-2} s^{-1}, and conductances in mol m^{-2} s^{-1} Pa^{-1} for the liquid phase and m s^{-1} for the gas phase, unless indicated otherwise. The most important variables and parameters are listed in Table 1.

[16] Figure 1 shows schematically the path of water for two scenarios (scenarios a and b) of water potential in soil, ψ_s, and air humidity, e_a. In Figure 1, the path of water is simplified into two steps: conduction from soil to leaf in the liquid phase and diffusion from leaf to the air in the gas phase. The step from soil to leaf includes the hydraulic resistances of roots, stems, and leaves, and the step from leaf to air includes the stomatal and aerodynamic resistance. The two steps are linked via the partial vapor pressure in the intercellular space e_i, which is in equilibrium with leaf water potential. In practice, leaf water potential is always such that e_i is near the saturated vapor pressure at leaf temperature, and thus, the effect of leaf water potential on e_i is negligible in the natural range of leaf water potential values [*Milly*, 1991].

[17] Had the conductances in the vegetation been constant, then leaf water potential would vary proportionally with soil water potential and atmospheric vapor pressure. However, vegetation actively adjusts conductances to keep water potentials within certain limits, in order to avoid the expansion of vacuum in xylem vessels, so-called embolism or cavitation [*Magnani et al.*, 2000; *Meinzer et al.*, 2001; *Mencuccini*, 2003]. There is evidence that for this reason conductances are adjusted such that during a growing season, relatively constant values for predawn leaf water potential result, despite order of magnitude differences in soil water potential and vapor pressure [*Zhang and Davies*, 1989; *Khalil and Grace*, 1992; *Whitehead et al.*, 1996]. The mechanism behind this phenomenon is that abscisic acid (ABA) produced by the roots in drying soil and transported to leaves reduces stomatal aperture [*Zhang et al.*, 1987]. The relatively constant leaf water potential holds only for predawn conditions. During the day leaf water potential decreases as a consequence of the time lag between root water uptake and transpiration and consequently changes in leaf water content [*Schulze et al.*, 1985; *Sperry et al.*, 2002]. To maintain constant leaf water potential on a seasonal timescale, the hydraulic and surface conductance should take values that are inversely proportional to the difference in potential between soil and leaf, and the difference between partial vapor pressure between leaf and air, respectively. If both soil water potential and partial vapor pressure are low (as in scenario a in Figure 1), the hydraulic conductance is high compared to the surface conductance. The opposite holds if both soil and air potential are high (as in scenario b).

[18] *Wong et al.* [1979] discovered a close relationship between photosynthesis rate and stomatal conductance under conditions of ample soil moisture and constant humidity deficit, resulting in a rather constant value of C_i of about 70

percent of the ambient concentration C_a for vegetation of the C3 photosynthetic pathway. The fact that both leaf water potential and internal carbon dioxide concentration are relatively constants suggests active regulation of the two conductances. Vegetation can adjust the two conductances in a number of ways, operating at different timescales.

[19] The hydraulic conductance can be adjusted by changing the root surface and sapwood area and vessel structure on the long term [*Magnani et al.*, 2000] and by embolism and repair after embolism on the short term [*Parsons and Kramer*, 1974; *Meinzer*, 2002; *Clarkson et al.*, 2000]. The stomatal conductance can be adjusted by changing the number of stomata, the stomatal pore length and the guard cell width on the long term [*Franks et al.*, 1998; *Hetherington and Woodward*, 2003] and by opening or closing stomata in response to quick changes of photosynthesis rate and humidity deficit on the short term (among others, *Meidner and Mansfield* [1968]).

[20] Distinguishing timescales is important. In this paper, three timescales are distinguished: (1) a short timescale (diurnal cycle) at which leaf water potential is flexible but most biochemical properties can be considered constant, (2) an intermediate timescale at which leaf water potential is maintained above the point of embolism and photosynthetic capacity and internal carbon dioxide concentration change but the architecture, biomass, and species composition remain constant (seasonal cycle), and (3) a long timescale at which all vegetation characteristics are flexible (multiple years or decades).

[21] *Cowan* [1977] and *Cowan and Farquhar* [1977] assumed that at the shortest timescale, stomatal regulation operates such that net photosynthesis is maximized for a particular amount of transpiration. This concept produces realistic diurnal cycles of fluxes of carbon dioxide and water [*Makela et al.*, 1996; *Arneth et al.*, 2002; *Van der Tol et al.*, 2007] but does not explain why parameters take certain values. This paper focuses on the intermediate and long timescales, in order to explain the most important parameters. This is the timescale at which leaves, roots, and sapwood are formed and nutrients are allocated.

[22] If water fluxes in the liquid phase from soil to leaf and in the vapour phase from stomata to air are equal, then transpiration rate E is

$$E = K(\psi_s - \psi_l) = 1.6gD \tag{2}$$

where $D = \frac{\rho_a}{M_a}\frac{e_i - e_a}{p}$ is the molar vapor gradient between stomata and the air (mol m^{-3}), e_i and e_a the vapor pressure in the intercellular spaces and in the ambient air (Pa), respectively, p atmospheric pressure (Pa), ρ_a specific mass of air (kg m^{-3}) and M_a the molar mass of air (kg mol^{-1}), and 1.6 the ratio of molecular diffusivity of water to that of carbon dioxide. The conductance for carbon dioxide is used rather than that of water to make a direct comparison with the carbon dioxide flux possible. Rearranging equation (2) [*Hubbard et al.*, 2001]:

$$g = \frac{\psi_s - \psi_l}{1.6D}K = \frac{E}{1.6D} \tag{3}$$

Parameter g also appears in the diffusion equation of carbon dioxide. Transport of carbon A on the trajectory between stomata and the air relates to the conductance g in the following way:

$$A = g(C_a - C_i) \tag{4}$$

Photosynthesis of C3 plants is described with the model of *Farquhar et al.* [1980]. Photosynthesis is either light or enzyme limited. For both conditions, the relationship between carbon dioxide concentration and photosynthesis is hyperbolic. Photosynthesis of C4 plants is described with the model of *Collatz et al.* [1992]. The two photosynthesis models are scaled from leaf to canopy level using the method described in Appendix A. Although the equations for C3 and C4 photosynthesis are different, they can at canopy level be described with the same equation, albeit using different parameter values. By scaling, the contributions of light and enzyme limited leaves are added. The resulting, effective relationship for the canopy as a whole is

$$A = \frac{\nu(C_i - \Gamma^*)}{C_i + \gamma} - R_{dd} \tag{5}$$

where ν is an (irradiance dependent) photosynthetic capacity (mol m^{-2} s^{-1}), γ is a shape factor (mol m^{-3}), Γ* is the carbon dioxide compensation point for photorespiration (mol m^{-3}), and R_{dd} is daytime dark respiration (mol m^{-2} s^{-1}). Parameter Γ* is zero for C4 plants. Parameter ν represents photosynthetic capacity integrated over the canopy and accounts for light limited leaves as well as light saturated leaves. The value of ν correlates positively with leaf nitrogen content [*Field and Mooney*, 1986, and references therein] and leaf area index [*Reich et al.*, 1999]. Owing to shadowing effects, ν at canopy scale cannot grow unlimited: an increase in leaf area index reduces the light interception by the lowest leaves and so does an increase in ν at leaf level, which requires thicker leaves. Consequently, the value of ν can be limited by light. Dark respiration includes carbon dioxide produced by maintenance and growth processes which leaves the canopy via the stomata. *Ryan* [1991] suggested to express dark respiration as a function of leaf nitrogen content. This concept was also applied by *Amthor* [1994], and indeed, *Reich et al.* [1998] found that dark respiration increases with both leaf nitrogen and specific leaf area for different functional groups in different biomes. This makes it reasonable to assume that dark respiration is proportional to photosynthetic capacity, that represents a true loss of carbon dioxide:

$$R_{dd} = m_d\nu \tag{6}$$

where m_d is a dimensionless maintenance coefficient. Using this in equation (5):

$$A = \nu\left(\frac{C_i - \Gamma^*}{C_i + \gamma} - m_d\right) \tag{7}$$

[23] Equation (4) describes the transport of carbon dioxide into the stomata, and equation (7) describes the consumption of carbon dioxide by photosynthesis. Examples of transport and photosynthesis calculated with these equations as a

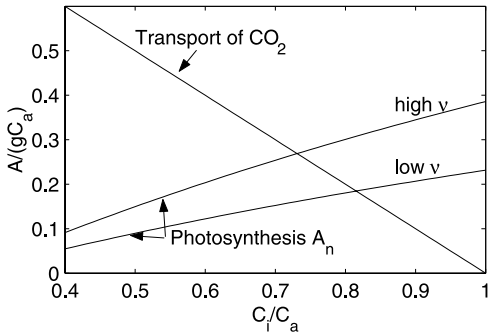

Figure 2. Net photosynthesis A for photosynthetic capacity $\nu = 75\ \mu\text{mol m}^{-2}\,\text{s}^{-1}$ (low ν) and $\nu = 125\ \mu\text{mol m}^{-2}\,\text{s}^{-1}$ (high ν), and transport of carbon dioxide by diffusion into the stomata, both scaled with gC_a, versus C_i/C_a, using $m_n = m_d = 0.07$. At the intersection, transport and consumption of carbon dioxide by photosynthesis are in equilibrium. Equilibrium concentration of carbon dioxide is negatively correlated with photosynthetic capacity ν.

function of internal carbon dioxide concentration are shown in Figure 2. Transport decreases and photosynthesis increases with increasing internal carbon dioxide concentration. At the intersection of the two curves, carbon dioxide concentration is in equilibrium. A higher photosynthetic capacity results in a lower equilibrium internal carbon dioxide concentration, and higher net assimilation (Figure 2).

[24] The relation between C_i and ν can be found by combining equations (4) and (7):

$$\nu = cg \tag{8}$$

where

$$c = \frac{C_a - C_i}{\frac{C_i - \Gamma^*}{C_i + \gamma} - m_d} \tag{9}$$

A similar expression, albeit excluding dark respiration, was derived by *Katul et al.* [2003].

[25] One remark can be made with this equation is that parameter C_i should be the actual, instantaneous value of internal carbon dioxide concentration. In the next sections we will use effective, long term values for C_i. One can see from equation (9) that the mean of c is not necessarily the same as c of the mean C_i.

[26] It is now important to focus on respiration. From Figure 2 one could conclude that the highest net assimilation rate is reached if ν approaches infinity. In reality, this does not occur for two reasons. First, photosynthetic capacity is limited by resources such as light and nutrients, and second, a higher photosynthetic capacity requires proportionally higher investment and maintenance costs. Our model does not account for this because by using net assimilation of leaves in the transport equation (equation (4)), other respiration terms are excluded and it is implicitly assumed that all respired carbon dioxide is recycled within the vegetation and directly available for carboxylation. This may be true for respiration in leaves during the day but not in nongreen tissue and not during the night. It is likely that part of the respired carbon dioxide is recycled and part is not [*Lloyd and Farquhar*, 1996]. It is assumed that an additional, nonrecycled, autotrophic respiration exists (night respiration and respiration of nongreen tissue), R_{dn}, proportional to photosynthetic capacity ν:

$$R_{dn} = m_n \nu \tag{10}$$

[27] Growth G is assimilation minus nighttime respiration:

$$G = A - R_{dn} = g(C_a - C_i) - gcm_n \tag{11}$$

where m_n is a nighttime canopy respiration coefficient. Parameter m_n is a coarse term for the trade-off between daytime growth and nighttime maintenance of the photosynthetic apparatus and maintenance of roots and stems. A higher photosynthetic capacity leads to both higher assimilation rates and higher respiration costs. It is the question which respiration components m_n should include. If growth of leaves only is considered, then leaf respiration should be included. If growth of whole individuals is considered, then respiration of all tissues should be included, of which leaf respiration is only a minor term. The principle remains the same in both cases, but the interpretation of m_n and G is different. This simplification has been used before by *Amthor* [1994], and *Cannell and Thornley* [2000] argue that on theoretical grounds, maintenance respiration is indeed closely related to tissue nitrogen content. Later, in the evaluation [*van der Tol et al.*, 2008], only growth of leaves is considered. For practical applications, allocation rules and parameters to include different respiration terms separately are needed in addition [*Cannell and Thornley*, 2000].

[28] We have now an expression for growth G. Conductance parameter g forms the connection with the transport of water. By combining equations (3), (8), and (11) and eliminating g:

$$\begin{aligned} G &= \frac{E}{1.6D}(C_a - C_i - cm_n) \\ \frac{\nu}{c} &= \frac{E}{1.6D} \end{aligned} \tag{12}$$

In the next section, equation (12) is used to calculate optimum parameters.

3. Optimum Biochemical Properties for Stationary Conditions

[29] In this section, optimum photosynthetic capacity and internal carbon dioxide concentration are calculated for a fixed g. In other words, the ratio $E/(1.6D)$ in equation (12) is prescribed. This implies the assumption that both D and E are climatic constraints. Transpiration E is then assumed to be limited by water availability.

[30] It is easier to use C_i instead of ν as an independent variable. Figure 3 shows $C_a - C_i$ and $m_n c$ as a function of C_i for a given g. Equation (11) says that the net growth is the difference between these two functions. Figure 3 shows that the difference reaches a maximum for the C_i where the tangent to $m_n c(C_i)$ has the same slope as $C_a - C_i$.

[31] The internal carbon dioxide concentration for which growth is maximized is found by solving:

$$\frac{dG}{dC_i} = 0 \tag{13}$$

Solving equation (11) for C_i, while keeping g constant (i.e., constant ψ_s, ψ_l, D and K), yields a quadratic equation, the

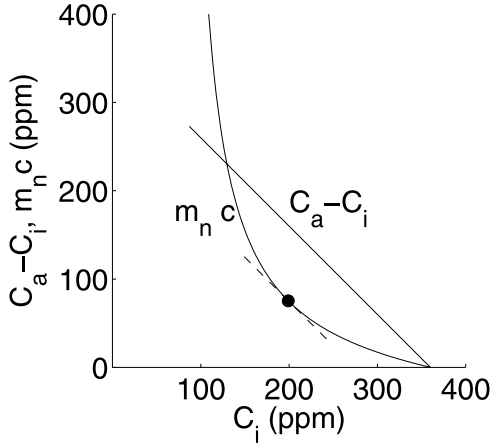

Figure 3. Finding the optimum C_i: the straight line, $C_a - C_i$, is proportional to cumulative gross carbon uptake, and the curved line, $m_n c$, to maintenance respiration. The maximum net carbon uptake occurs were the difference between the lines is the largest. This is the case where the derivatives of the lines equal.

positive solution of which is the optimal internal carbon dioxide concentration $C_{i\mathrm{opt}}$ at which growth is maximized:

$$C_{i\mathrm{opt}} = \frac{-a_1 + \sqrt{a_1^2 - 4a_2 a_0}}{2a_2} \tag{14}$$

where

$$a_0 = m_n\{(\Gamma^* + m_d\gamma)(\gamma - C_a) - (1 - m_d)C_a\gamma\} + (\Gamma^* + m_d\gamma)^2$$

$$a_1 = 2(\Gamma^* + m_d\gamma)(m_n - (1 - m_d))$$

$$a_2 = m_n(m_d - 1) + (1 - m_d)^2$$

Now optimum photosynthetic capacity is calculated with equation (8).

[32] Optimum internal carbon dioxide concentration depends on the respiration terms (photorespiration and dark respiration during the day and night) but not on conductance g, whereas optimum photosynthetic capacity is proportional to g. For common values of the parameters for C3 vegetation (C_a = 360 ppm, Γ^* = 30 ppm, γ = 700 ppm, $m_d = m_n$ = 0.04 to 0.12), optimal C_i/C_a is between 0.5 and 0.8, and for C4 vegetation (C_a = 360 ppm, Γ^* = 0 ppm, γ = 55 ppm, $m_d = m_n$ = 0.15 to 0.30 [*Collatz et al.*, 1992; *Sellers et al.*, 1996], optimal C_i/C_a is between 0.25 and 0.5. These values are in the range of literature values [*Lloyd and Farquhar*, 1994]. The choice of the values for parameters m_d and m_n for C3 vegetation is discussed in the work of *van der Tol et al.* [2008].

[33] Figure 4 shows the dependence of optimal C_i on temperature and ambient oxygen concentration, calculated with equation (14), in which Γ^* and γ for enzyme limited photosynthesis are calculated as functions of temperature and oxygen concentration according to *Farquhar et al.* [1980]. The values for C_i are slightly lower than most literature values [*Lloyd and Farquhar*, 1994]. This may be explained by the fact that only stationary conditions are considered here. It is shown later that the optimum values of C_i in nonstationary conditions are higher and more realistic. The dependence of $C_{i\mathrm{opt}}$ on temperature and oxygen concentration qualitatively agrees with observations of *Korner et al.* [1991], who found that variations in internal carbon dioxide concentration along gradients of altitude and latitude could be explained from variations in temperature and atmospheric pressure. They found that C_i increases while moving from high altitude at low latitude to low altitude at high latitude (from low to high pressure at constant temperature), and while moving from a high to a low latitude at constant altitude (from low to high temperature). Similarly, *Sparks and Ehleringer* [1997] observed an increase in C_i while moving from high to low altitude (from low temperature and low pressure to high temperature and high pressure). *Farquhar and Wong* [1984] observed an increase in C_i/C_a with increasing oxygen concentration at constant ambient carbon dioxide concentration.

[34] Hitherto stationary conditions have been considered, in which g is known. In that case, C_i is independent of g, and ν is a linear function of g. A constant g is not realistic, and for that reason, g is modelled as a function of soil moisture content in the next section.

4. Optimum Biochemical Properties During a Dry Season

[35] Soil water potential and humidity have seasonal cycles and interannual and random fluctuations. In this section, the seasonal cycle of transpiration is modelled as a function of soil moisture content. Now, not only optimum photosynthetic capacity and internal carbon dioxide concentration but also the optimum seasonal cycle of transpiration is calculated. A simple differential equation for a soil reservoir is introduced. It is assumed that the dry period is long enough to affect the biochemical processes in the vegetation but too short for the vegetation to change biomass and respiration (intermediate timescale). Factors that can influence medium timescale biochemical processes are soil water potential, temperature, and radiation during a season.

[36] During a dry season, soil water potential may easily vary over two orders of magnitude. Various ways exist in which vegetation handles conditions of drought, often classified as measures of avoidance and tolerance. Here, we only calculate the optimum strategy, without going into details of how they physiologically work. Transpiration and surface conductance in water limited conditions, for constant vapour pressure deficit, are written as:

$$\begin{aligned} E &= \xi E_0 \\ g &= \xi g_0 \end{aligned} \tag{15}$$

where E_0 and g_0 are the transpiration rate and surface conductance in unstressed conditions, and ξ a stress response function, defined as:

$$\xi = \frac{E}{E_0} = \frac{K(\psi_s - \psi_l)}{K_0(\psi_{s0} - \psi_{l0})} \tag{16}$$

where K_0, ψ_{s0} and ψ_{l0} are hydraulic conductivity, soil and leaf potential in unstressed conditions. In equation (15) it is implicitly assumed that vapor pressure deficit is constant during the season. Unlike soil moisture content, the evolution of vapor pressure deficit is not modelled because it depends on many (regional) factors which cannot be

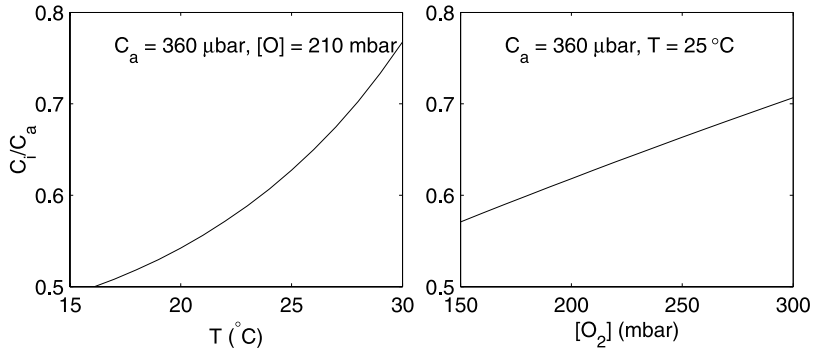

Figure 4. Modelled optimal internal carbon dioxide concentration versus temperature at constant ambient oxygen and carbon dioxide concentration and versus oxygen concentration for constant temperature and ambient carbon dioxide concentration, calculated with equation (14) for enzyme limited conditions, $m_n = m_d = 0.06$, and using Arrhenius functions for the temperature-dependent Michaelis-Menten coefficients.

included in a simple model. Consequently, parameter D represents the effect of atmospheric demand integrated over the season. Possible effects of this simplification are discussed in the last section. In the evaluation of the model, measured vapor pressure deficit is used, and thus any feedback between transpiration and vapor pressure deficit is already included in the model input.

[37] Equation (16) is rather impractical for climate models because the functions $K(\psi_s)$ and $\psi_l(\psi_s)$ are usually not known. In this study it is replaced with an empirical equation, in which ξ is a function of soil moisture content or soil water storage. The empirical expression for ξ as a function of soil moisture content θ is

$$\begin{aligned} \xi &= 1 \quad \text{for} \quad \theta \geq \theta_f \\ \xi &= \left\{ \frac{\theta - \theta_r}{\theta_f - \theta_r} \right\}^{\alpha} \quad \text{for} \quad \theta < \theta_f \end{aligned} \tag{17}$$

where θ_r and θ_f are the soil moisture content at wilting point and at the point below which transpiration is reduced, respectively, and α an empirical, species and soil dependent shape factor. This parameterization is often used in the literature, with the linearity assumption: $\alpha = 1$ [e.g., *Laio et al.*, 2001; *Albertson and Kiely*, 2001; *Daly et al.*, 2004a, 2004b]. Since the linearity assumption is sometimes empirically found to predict a too low ξ, we consider in this section a more general expression with α unfixed.

[38] The soil moisture content is replaced by amounts of available soil water s in excess of the amount of water at wilting point (mol m^{-2}, but this can easily be converted into the more conventional unit of millimeters, using molecular weight and density of water):

$$\xi = \min(1, \sigma^{\alpha}) \tag{18}$$

where $\sigma = \left(\frac{s - s_r}{s_f - s_r}\right)$, s_f is the amount of water in the soil below which water stress starts and s_r the amount of water in the root zone at wilting point.

[39] The corresponding evolution of $s(t)$ during a long dry period is as follows. Since there is no recharge,

$$\frac{ds}{dt} = -E(t) \tag{19}$$

where t is time. Initially, transpiration is unstressed as sufficient water is available. The available amount is s_0 (mol m^{-2}, or millimeters) is the amount of water in the root zone. At time $t = t_f$, water stress starts. Time t_f is the time at which soil water storage s reaches s_f:

$$t_f = \frac{s_0 - s_f}{1.6 g_0 D} \tag{20}$$

After t_f, transpiration is reduced, and then the evolution of σ can be calculated by using equation (18) in equation (19):

$$\frac{d\sigma}{dt} = -\frac{E}{s_f - s_r} = -\frac{1.6 D g_0 \sigma^{\alpha}}{s_f - s_r} \tag{21}$$

The solution of this differential equation (with initial condition $\sigma(t_f) = 1$) is

$$\begin{aligned} \sigma(t) &= \left(1 - (1-\alpha)\frac{1.6 D g_0}{s_f - s_r} t + (1-\alpha)\frac{s_0 - s_f}{s_f - s_r}\right)^{1/(1-\alpha)} \quad \text{for } \alpha \neq 1 \quad \text{(a)} \\ \sigma(t) &= \exp\left(-\frac{1.6 D g_0 t - (s_0 - s_f)}{s_f - s_r}\right) \quad \text{for } \alpha = 1 \quad \text{(b)} \end{aligned} \tag{22}$$

The evolution of the stress response function is $\xi(t) = \sigma(t)^{\alpha}$. $E(t)$ and $g(t)$ can be calculated with equation (15).

[40] Now we turn to the consequent effect of water stress on the biochemical parameters ν and C_i. By combining with equation (8):

$$\frac{\nu}{c} = \xi \frac{\nu_0}{c_0} \tag{23}$$

where ν_0 and c_0 are values for ν and c in unstressed conditions. Thus, in case of water stress ($\xi < 1$), the parameters for photosynthesis are forced to change: either photosynthetic capacity ν or internal carbon dioxide concentration C_i decreases. The two options are two fundamentally different mechanisms: decreasing photosynthetic capacity implies an inhibition of metabolism [*Keck and Boyer*, 1974; *Younis et al.*, 1979; *Gimenez et al.*, 1992; *Wilson et al.*, 2000], whereas decreasing internal carbon

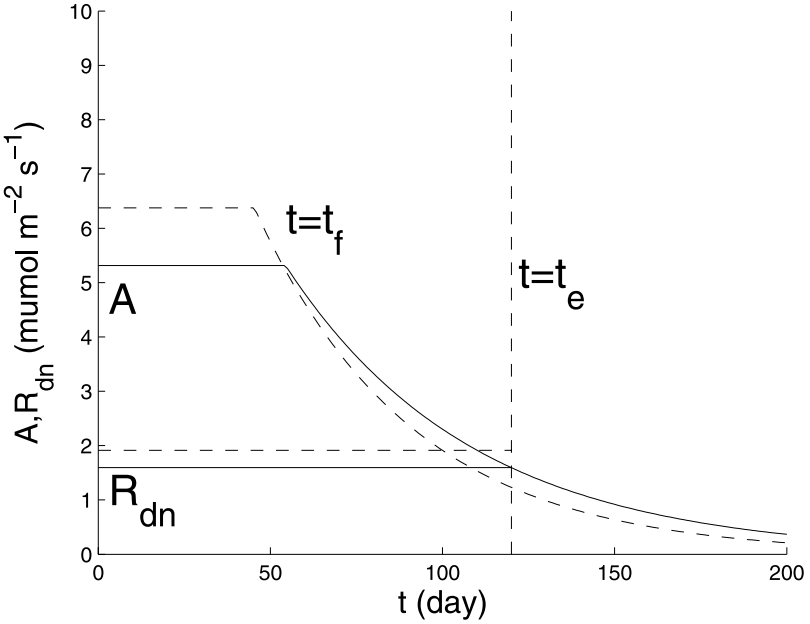

Figure 5. Evolution of the assimilation A and nonrecycled respiration R_{dn} before and after water stress. Water stress starts at t_f, while t_e is the assumed end of the drought period (thereafter A is virtual, but the tail plays a role in the theory). The dashed lines correspond to a higher unstressed conductance than the solid lines.

dioxide concentration implies only a reduction of diffusion of carbon dioxide into the stomata as a result of partial stomatal closure [*Brestic et al.*, 1994; *Quick et al.*, 1992; *Damesin et al.*, 1998]. Most evidence points towards an inhibition of metabolism caused by a decrease of Rubisco regeneration [*Gimenez et al.*, 1992; *Gunasekera and Berkowitz*, 1993], Rubisco activity [*Castrillo and Calcagno*, 1989; *Medrano et al.*, 1997] or ATP synthesis [*Tezara et al.*, 1999]. *Medrano et al.* [2002] gave evidence that the stomatal mechanism prevails during moderate water stress and the inhibition of metabolism during severe water stress. Experimental data presented in the companion paper also promote the idea that the reduction of photosynthesis during a season is mainly related to the inhibition of metabolism. In this study, it is assumed that on a seasonal timescale, photosynthetic capacity responses to drought, while C_i remains constant. As a consequence, equation (4) becomes

$$A(t) = (C_a - C_i)g(t) \tag{24}$$

with $(C_a - C_i)$ time-independent.

[41] The question is now to find the unstressed photosynthetic capacity ν_0 and c_0 (or C_i) for which growth is maximized. It can intuitively be expected that the longer the expected duration of the dry period, the lower the initially unstressed transpiration rate in order to save water in anticipation of a long dry period. *Makela et al.* [1996] used a model for optimal stomatal control during dry periods of stochastic duration, and the assumption that vegetation aims to maximize cumulative growth. They indeed found that the initial transpiration rate decreases with the expected duration of the dry period. The approach followed here is different because both photosynthetic capacity and internal carbon dioxide concentration are optimized, whereas in their model, photosynthetic capacity had a fixed a priori value, and only stomatal regulation was optimized.

[42] The seasonal cycles of surface conductance, transpiration and assimilation as functions of photosynthetic capacity and internal carbon dioxide concentration, have been derived above. Next, the cumulative net carbon gain during the season is calculated. The optimum conditions are those for which cumulative carbon gain is maximized with respect to photosynthetic capacity and internal carbon dioxide concentration.

[43] The total cumulative growth or carbon fixation during such a season Q is found by integrating carbon yield over the season. It is assumed that internal carbon dioxide concentration and nonrecycled respiration remain constant during the season, and respiration is proportional to the photosynthetic capacity in unstressed conditions ν_0. Evidence for the assumption of a constant rate of nonrecycled respiration is presented in the work of *van der Tol et al.* [2008]. Using these assumptions:

$$\begin{aligned} Q &= \int_0^{t_e} (A(\tau) - R_{dn}(\tau))d\tau \\ &= (C_a - C_i)\left(\frac{s_0 - s_f}{1.6D} + \int_{t_f}^{t_e} g(\tau)d\tau\right) - m_n c g_0 t \end{aligned} \tag{25}$$

Using the fact that

$$g = \frac{E}{1.6D} = -\frac{1}{1.6D}\frac{ds}{dt} = -\frac{s_f - s_r}{1.6D}\frac{d\sigma}{dt} \tag{26}$$

yields for the integral after t_f:

$$\int_{t_f}^{t} g(\tau)d\tau = \frac{s_f - s_r}{1.6D}(1 - \sigma(t)) \tag{27}$$

[44] Let us now illustrate this. Figure 5 shows $A(t)$ and R_{dn}. Their time integrals Q_A and Q_{Rdn} are the areas below

the respective curves, to the left of $t = t_e$. The amount of water uptake is proportional to the area below $A(t)$ because of equations (24) and (2), and because D and C_i were kept constant. Figure 5 shows what happens when g_0 is increased. The initial $A(t)$ is proportional to g_0, but t_f falls since the area below the straight part of A corresponds to a water uptake which is fixed at $s_0 - s_f$. After stress has begun, $A(t)$ drops faster for larger g_0. The entire area below $A(t)$ from $t = 0$ to infinity corresponds to the uptake of all the available water, $s_0 - s_r$, and remains constant while g_0 varies. This is the limit value for Q_A; the actual Q_A is this value minus the area of the tail after $t = t_e$. The tail corresponds to water uptake $(s_f - s_r)\,\sigma(t_e)$. So the total Q is

$$Q = Q_{A,limit} - \frac{C_a - C_i}{1.6D}(s_f - s_r)\sigma(t_e) - m_n c g_0 t_e \tag{28}$$

Optimizing equation (28) with respect to g_0, while keeping C_i and t_e constant, leads to:

$$\frac{dQ}{dg_0} = 0 = (C_a - C_i)\xi(t_e)t_e - m_n c t_e \tag{29}$$

In the derivation of equation (29) it has been used that $Q_{A,limit}$ is constant, that $d\sigma/dg_0 = -1.6\,Dt_e\sigma^{\alpha}/(s_f - s_r)$ for $t = t_e$, and that $\xi = \sigma^{\alpha}$ for $t_e > t_f$. From equation (29) follows that $\xi(t_e) = 1/r$ in which

$$r = \frac{A_0}{R_{dn}} = \frac{C_a - C_i}{m_n c} \tag{30}$$

is the ratio of assimilation to nonrecycled respiration. This implies that the optimum $A(t)$ has the property $A(t_e) = A_0/r = R_{dn}$ as illustrated in Figure 5. The optimum solution for g_0 is found by solving g_0 from $\sigma(t_e)^{\alpha} = 1/r$, and is

$$\begin{aligned} g_{0opt} &= \frac{s_f - s_r}{1.6Dt_e}\left(\frac{1 - r^{1-1/\alpha}}{1-\alpha} + \frac{s_0 - s_f}{s_f - s_r}\right) \quad \text{for } \alpha \neq 1 \quad \text{(a)} \\ g_{0opt} &= \frac{s_f - s_r}{1.6Dt_e}\left(\ln r + \frac{s_0 - s_f}{s_f - s_r}\right) \quad \text{for } \alpha = 1 \quad \text{(b)} \end{aligned} \tag{31}$$

from which the optimum initial transpiration E_{0opt}, photosynthetic capacity ν_{0opt} and assimilation rate A_{0opt} can be calculated easily:

$$\begin{aligned} E_{0opt} &= 1.6Dg_{0opt} \\ \nu_{0opt} &= cg_{0opt} \\ A_{0opt} &= (C_a - C_i)g_{0opt} \end{aligned} \tag{32}$$

[45] We have now derived an optimum shape of the seasonal cycle of transpiration for a not recharged reservoir of soil water. Like in the stationary case, optimum photosynthetic capacity is proportional to g in unstressed conditions, but now g decreases with time as drought progresses.

[46] Figure 5 clearly illustrates the dilemma: if the initial photosynthesis rate is high, then a large portion of available water is transpired, and gross photosynthesis is high. However, a high initial photosynthesis rate also implies a stronger reduction of photosynthesis by stress later during the season and relatively high respiration losses.

[47] The decline of transpiration as a result of drought is described by the term $\xi(t)$. The optimum shape of $\xi(t)$ is a function of internal carbon dioxide concentration, the duration of the dry period and respiration. This is best illustrated in the special case in which water stress occurs already at the start of the growing season ($s_0 = s_f$) and transpiration is linearly proportional to the amount of available water ($\alpha = 1$). Then:

$$\xi(t) = \mathrm{e}^{-\ln r\frac{t}{t_e}} \tag{33}$$

This equation shows that the tail of the transpiration curve during the dry season depends on two parameters: the duration of the dry period t_e and the ratio of assimilation to nonrecycled respiration r. The effect of 1/ln r on the shape of ξ is equivalent to the effect of t_e. The ratio r increases with increasing C_i (r is the right-hand side of equation (7) but with "ν" replaced with "$1/m_n$") because at a higher C_i, the photosynthetic capacity is used more efficiently. A high C_i is brought about by fixing ν_0/g_0 at a low value. On the other hand, a lower C_i (higher ν_0/g_0) has a similar effect on ξ as a longer duration of the dry period t_e. Both correspond to a more conservative use of water.

[48] Thus the model predicts that vegetation with a high internal carbon dioxide concentration has a higher transpiration rate in unstressed conditions but is more sensitive to drought than vegetation with a low internal carbon dioxide concentration. This prediction agrees with observations by *Ehleringer* [1993], who found that vegetation with a high C_i grows faster than vegetation with a low C_i when stress is removed, while vegetation with a low C_i is more resistant to drought.

[49] The optimal internal carbon dioxide concentration C_i can be calculated by solving:

$$\frac{dQ}{dC_i} = 0 \tag{34}$$

while using the derived expression for $\nu_0 = \nu_{0opt}$. An analytical solution of equation (34) is rather complicated. The optimum C_i is higher than in the stationary case in which no water stress occurs. The reason lays in the assumption that assimilation decreases in case of stress, but respiration does not. In order to avoid relatively large respiration losses, C_i should be higher. This point can also be illustrated as follows. As $A(t) = g_0\xi(t)(C_a - C_i)$, we can rewrite the accumulated net growth as:

$$Q = g_0 t_e[\xi_{av}(C_a - C_i) - m_n c], \tag{35}$$

in which ξ_{av} is the time average of the stress response function $\xi(t)$ from $t = 0$ to $t = t_e$. Treating for simplicity g_0 as a constant (instead of ν_0), we see that this is maximized if the expression between the square brackets is maximized. In the previous section this problem was solved for no drought ($\xi_{av} = 1$). For $\xi_{av} < 1$ it can again be solved graphically using Figure 3, but now we should multiply the line $(C_a - C_i)$ with shrinking factor ξ_{av}. One sees that the difference between the new curves is maximal for a $C_{i,opt}$ which is larger than the old (unstressed) one, and the more as average

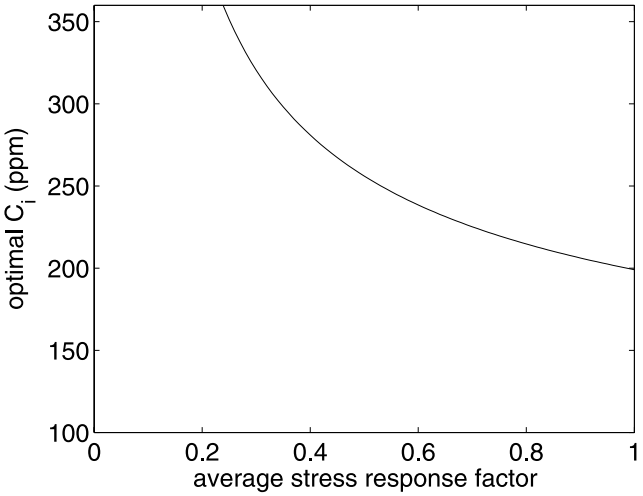

Figure 6. Response of the modeled optimal internal CO_2-concentration C_i to the average stress response factor ξ_{av}. The upper limit for C_i is C_a (=360 ppm).

stress ξ_{av} drops farther below 1. Figure 6 illustrates the dependence of $C_{i\ opt}$ on ξ_{av}. The increase of C_i requires of course a decrease of ν_0/g_0.

[50] The above set of equations provides optimum photosynthetic capacity, internal carbon dioxide concentration and transpiration in conditions of drought. Optimum C_i can be calculated by solving equation (34) numerically. One remarkable feature is, that the lower the value for $\frac{s_f - s_r}{s_0 - s_r}$, the lower optimum C_i. This would mean that the higher the availability of water s_0 (at constant s_f), the lower the optimum C_i. This is contrary to some studies, which show a positive relation between water availability and C_i [*Meinzer et al.*, 1992]. In the next section, the optimality hypothesis will be discussed and alternatives presented, which explains why this contradiction occurs. Another interpretation is that the lower the value for s_f at constant s_0 (i.e., water stress starts at a lower soil moisture content), the lower the optimum C_i, which implies that drought resistant vegetation has a lower optimum C_i.

5. Biochemical Properties in a Variable Climate

[51] This section addresses the issue of the stochastic nature of environmental conditions and the assumption that vegetation characteristics are such that growth is maximized. It was previously assumed that for a dry season, photosynthetic capacity and internal carbon dioxide concentration can be chosen freely. In reality, conditions during a single season may be too short for the vegetation to adapt to. The vegetation carries a memory of the climate of previous seasons. The weather conditions during these seasons are of a stochastic nature. A way to deal with this stochastic nature of climate variables is by considering expected growth rates and chances of survival. Expected carbon fixation $\hat{Q}$ can be calculated as:

$$\hat{Q} = \int p(\tau) Q(\tau) d\tau \tag{36}$$

where $p(\tau)$ is the probability density function of an environmental variable, such as the duration of a dry period or the amount of available water and the integration runs over the domain of all possible values. It is possible to produce a map of expected carbon fixation $\hat{Q}$ for any combination of photosynthetic capacity and internal carbon dioxide concentration for some climate. Figure 7 shows such a map, for (left) simulations of $\hat{Q}$ for many combinations of ν_0 and C_i and (right) the probability of negative carbon fixation for stochastic water availability. The probability of negative carbon fixation is a measure for the risk of the vegetation: negative growth over a season may cause mortality (note that we speak here of carbon gain at canopy level; the situation for individuals may be different). In the simulations, water availability had a log-normal distribution with mean of the logarithmic of $s_0 - s_r$ of log(250 mm) and standard deviation of log(400/200), and $\hat{Q}$ was calculated by numerical integration over the probability density function (equation (36)). It was further

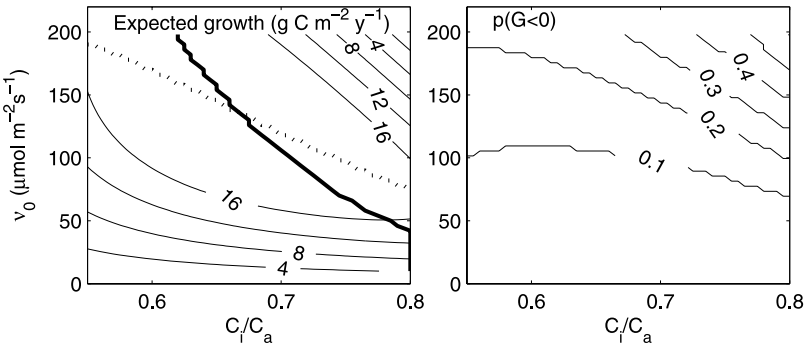

Figure 7. Expected seasonal cumulative carbon fixation $\hat{Q}$ (moles of CO_2 per m^2 per growing season) for (left) pairs of ν_0 and C_i/C_a (C_a = 360 ppm) and (right) the corresponding probability of a negative Q, for a dry season of 100 d with a variable initial soil water storage. A log-normal distribution was used for water availability with log(mean($s_0 - s_r$)) = log(250) and a standard deviation of log(400/200), $m_d = m_n = 0.05$, and $s_f - s_r$ = 150 mm. The bold solid line gives for any ν_0, the corresponding C_i for which growth is maximized (i.e., $\frac{\partial Q}{\partial C_i} = 0$), and the bold dashed line for any C_i, the value of ν_0 for which growth is maximized (i.e., $\frac{\partial Q}{\partial \nu_0} = 0$).

assumed that $s_f - s_r = 150$ mm and $m_d = m_n = 0.05$ and $\alpha = 1$. The bold solid line is the solution of the partial differential equation $\frac{\partial \hat{Q}}{\partial C_i} = 0$, and the dashed line $\frac{\partial Q}{\partial \nu_0} = 0$. The dashed line gives for any value of C_i, the value of ν_0 for which growth is maximized. Likewise, the solid line gives for any value of ν_0, the value of C_i for which growth is maximized. The optimum combination of carbon dioxide concentration is that at the intersection of the two lines.

[52] Vegetation characteristics are affected by metabolic processes, competition, mortality, and succession, limitation by various resources, pests, and diseases, and carry a history of previous events. It is assumed that the outcome of all these processes are vegetation characteristics that result in maximum growth but without any proof that this is indeed the case. As an alternative, let us consider a simple growth model, in which parameter ν_0 cannot be chosen freely but is a function of cumulative growth over the previous years. Assume that a bare field gets overgrown with vegetation. Initially, leaf area index is low, resulting in a low canopy photosynthetic capacity ν_0 (although photosynthetic capacity at leaf scale may be higher than for mature vegetation). Each year, biomass is incremented with a value proportional to carbon fixation Q of the previous year. If it is assumed that leaf area index increases proportionally, then ν_0 develops from a low to a high value. Consequently, the photosynthetic capacity ν_0 and internal carbon dioxide concentration may roughly follow the bold solid line in Figure 7, while C_i makes excursions to the left of this line during dry and excursions to the right during wet years. While vegetation grows, optimum internal carbon dioxide concentration decreases. Annual growth initially increases until the intersection of the bold and the dashed line is reached and then decreases again. This simple model explains why internal carbon dioxide concentration in pioneer vegetation is higher than in secondary vegetation and why pioneer vegetation has a more rapid growth but is less water efficient than secondary vegetation [e.g., *Donovan and Ehleringer*, 1994]. Let us further assume that photosynthetic capacity continues to increase until growth diminishes and vegetation reaches the climax biomass. If growth of photosynthetic capacity is limited by other resources than water, such as nutrients, then climax photosynthetic capacity is lower and internal carbon dioxide concentration higher than can be expected from Figure 7. This suggests that the eventual value of C_i at maximum biomass depends on which resource limits biomass: if it is water, then C_i is lower than if it is another resource.

[53] This concept is an oversimplification, used only to illustrate the fact that the ecologic optimality hypothesis used in this study does not take into account physiologic limitations to the parameters. In reality, the way photosynthetic capacity and internal carbon dioxide concentration develop in time and respond to variations between years also depend on their plasticity. For example, as vegetation growths taller, the hydraulic conductance reduces for physiological reasons [*Magnani et al.*, 2000].

6. Discussion and Conclusions

[54] An analytical model was presented to predict optimum vegetation characteristics. This model was inspired by concepts which have been developed and published in recent years. The current model for the first time successfully combines calculations of optimum photosynthetic capacity and internal carbon dioxide concentration by using the concept of homeostatic water transport. The optimum parameters reflect a strategy to deal with two trade-offs: the trade-off between fast growth and avoidance of drought and between a high photosynthetic capacity and avoidance of high respiration losses.

[55] In order to present the concepts clearly, analytical equations were used. The simplicity of the model also has a disadvantage: although the parameters have a conceptually clear meaning, the translation to commonly used parameters is indirect. For example, the calculated hydraulic and surface conductance do not equal their equivalents at an hourly timescale. Appendix A illustrated the consequences for scaling the photosynthesis model from leaf to canopy level: the responses of photosynthesis to light and carbon dioxide concentration change when moving from leaf to canopy scale and when averaging over a day or longer.

[56] An example of a drawback of a simple model is the treatment of vapor pressure deficit as a constant. In principle, a relationship between transpiration and vapor pressure deficit can be incorporated in the model in a similar way as the relationship between soil moisture content and transpiration. A negative feedback between transpiration and vapor pressure deficit enhances growth in unstressed conditions and reduces it in stressed conditions. However, it is in general unclear what the relationship is and to what extent it is a local feedback. In this study, vapor pressure deficit was a parameter for consistent differences in humidity between sites.

[57] The description of respiration by the model may need further attention in future studies. Compared to photosynthesis, respiration is modelled in a rather simple way. Although it is common practice to scale respiration with leaf nitrogen content or photosynthetic capacity [*Thornley and Cannell*, 2000], it is unlikely that the ratio of respiration to photosynthetic capacity is uniform in space. Moreover, it is unclear how much of the respired carbon is recycled. The model is sensitive to parameters m_d and m_n and may thus benefit from future improvements in the understanding of respiration.

[58] In the transport equations, it was assumed that water and carbon dioxide travel the same path. In reality, carbon dioxide is transported further into the mesophyll where the Calvin cycle takes place. In the model it is assumed that mesophyll conductance is infinite. One can model the effect of mesophyll conductance by introducing a correction factor for the ratio of mesophyll to stomatal conductance. A variable mesophyll conductance could play a role [*Warren and Adams*, 2006], but this is most likely a very minor effect that is ignored here for simplicity.

[59] This study is a first attempt to describe both the productivity and water use efficiency of vegetation from climatic constraints. Vegetation parameters are the result of a vast number of processes and nonlinear interactions. Parameter values are not only constrained by the history of availability of resources but also by an often unknown history of incidents such as fires or diseases. It is attractive to use an optimality hypothesis because it is intuitively plausible and mathematically easy to apply and has successfully been applied in many ecohydrological studies [*Field*, 1983; *Hirose and Werger*, 1987; *Makela et al.*, 1996]. One should keep in mind that the theory described

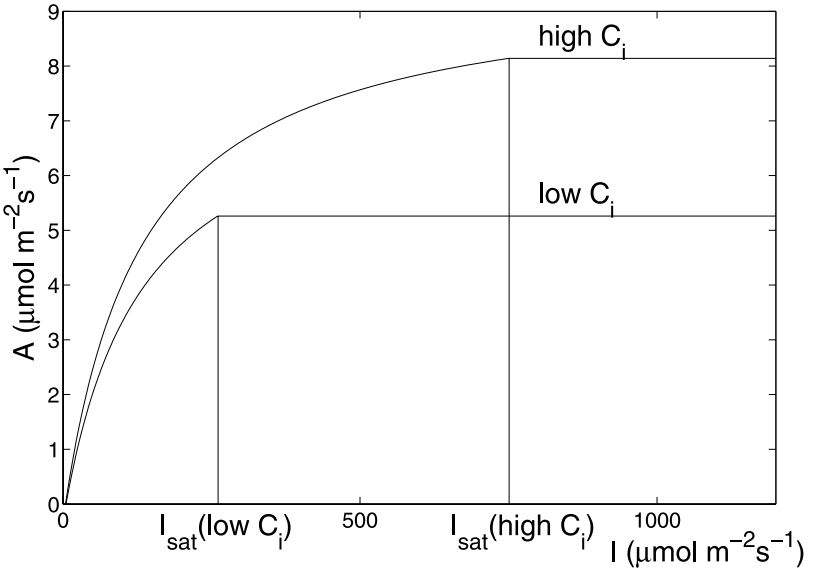

Figure A1. Schematic view of light response curves of assimilation (assimilation A versus irradiance I) at low and high internal carbon dioxide concentration C_i, and the corresponding lowest light levels at which assimilation of light saturated (I_{sat}).

in this paper sets general boundary conditions for growth, and does not consider other limitations that occur locally.

Appendix A: Upscaling of the Leaf Photosynthesis Model to Canopy Level

[60] Photosynthesis of vegetation of the C3 photosynthetic pathway is either light or enzyme limited. The equations for both cases can be described as:

$$A_c = \nu_c \frac{C_i - \Gamma^*}{C_i + \gamma} \tag{A1}$$

$$A_j = \nu_j(I) \frac{C_i - \Gamma^*}{C_i + \gamma_j} \tag{A2}$$

where A_c and A_j are canopy photosynthesis in the enzyme and light limited case, respectively. In a canopy, part of the leaves will be light limited and part light enzyme limited. The proportions of light saturated and light limited leaves change with time. Effective photosynthesis of a canopy can be described as:

$$A = p(I > I_{sat})A_c + \int_{I=0}^{I=I_{sat}} p(I)A_j(I)dI \tag{A3}$$

where p is the probability of irradiance on a leave to have a certain value, and I_{sat} is the intensity of irradiance above which photosynthesis is light saturated. Figure A1 illustrates that the value of I_{sat} is a function of C_i. Using equations (A1) and (A2), equation (A3) can be rewritten as:

$$A = \varepsilon(C_i, I)\nu_c \frac{C_i - \Gamma^*}{C_i + \gamma} \tag{A4}$$

Parameter ε takes a value between 0 and 1:

$$\varepsilon = p(I > I_{sat}) + \frac{C_i + \gamma}{C_i + \gamma_j} \int_{I=0}^{I=I_{sat}} p(I) \frac{\nu_j(I)}{\nu_c} dI \tag{A5}$$

[61] Owing to the fact that $\gamma > \gamma_j$, the term $\frac{C_i+\gamma}{C_i+\gamma_j}$ decreases with increasing C_i, and I_{sat} increases with increasing C_i. As a result, ε decreases with increasing C_i. However, in the range of natural values of C_i between 0.5 and 0.8, the sensitivity of ε to C_i is only small. As a first approximation, a constant value for ε can be used.

[62] Finally, we define an effective photosynthetic capacity at canopy scale as:

$$\nu = \varepsilon\nu_c \tag{A6}$$

For vegetation of the C4 photosynthetic pathway, the equations are different, but the result at canopy scale can be written in the same form, albeit with different parameter values. Photosynthesis is the minimum of electron limited (A_j), enzyme limited (A_j), and carbon dioxide limited photosynthesis (A_s). They can be written as [*Collatz et al.*, 1992; *Sellers et al.*, 1996]:

$$\begin{aligned} A_j &= \nu_j(I) \\ A_c &= \nu_c \\ A_s &= kC_i \\ k &= 2 \cdot 10^4 \nu_c / p \end{aligned} \tag{A7}$$

where p is atmospheric gas concentration (μmol m^{-3}). The transition between enzyme limited and carbon dioxide limited photosynthesis is smooth. Fitting a hyperbolic curve through the minimum of V_{cc} and V_{cs} results in

$$\min(A_c, A_s) = \frac{\nu_c \cdot C_i}{\gamma + C_i} \tag{A8}$$

where

$$\gamma = p/2 \cdot 10^4 \tag{A9}$$

[63] Equation (A8) can be used as the equivalent of the hyperbolic equation for A_c of the C3 model. A_j does not

depend on carbon dioxide or oxygen concentration due to the absence of photorespiration. Following the same reasoning as for C3 vegetation, we can again derive equation (A4) but using $\Gamma^* = 0$, $\gamma_j = 0$, and $\gamma = 2 \cdot 10^4 \nu_c/p \approx 55$ ppm.

[64] **Acknowledgments.** The authors thank the two anonymous reviewers, Andrew Friend, Franco Miglietta, Mark Bierkens, Karin Rebel, and Sampurno Bruijnzeel for their valuable comments.

References

Albertson, J. D., and G. Kiely (2001), On the structure of soil moisture time series in the context of land surface models, *J. Hydrol.*, *243*, 101–119.

Amthor, J. S. (1994), Higher plant respiration and its relationships to photosynthesis, in *Ecophysiology of Photosynthesis*, edited by E. Schultze and M. Caldwell, pp. 71–101, Springer, Berlin.

Arneth, A., J. Lloyd, H. Šantrůčková, M. Bird, S. Grigoryev, Y. N. Kalschnikov, G. Gleixner, and E.-D. Schulze (2002), Response of central Siberian Scots Pine to soil water deficit and long-term trends in atmospheric CO_2 concentration, *Global Biogeochem. Cycles*, *16*(X), 1005, doi:10.1029/2000GB001374.

Baldocchi, D. D., K. B. Wilson, and G. Lianhong (2002), How the environment, canopy structure and canopy physiological functioning influence carbon, water and energy fluxes of a temperate broad-leaved deciduous forest-an assessment with the biophysical model, *Tree Physiol.*, *22*, 1065–1077.

Brestic, M., G. Cornic, M. Fryer, and N. Baker (1994), Does photorespiration protect the photosynthetic apparatus in french bean leaves from photoinhibition during drought stress?, *Planta*, *196*, 450–457.

Cannell, M. G. R., and J. H. M. Thornley (2000), Modelling the components of plant respiration: Some guiding principles, *Ann. Bot.*, *85*, 45–54.

Castrillo, M., and A. M. Calcagno (1989), Effects of water stress and rewatering on ribulose 1,5-bisphosphate carboxylase activity, chlorophyll and protein contents in two cultivars of tomato, *J. Horticultural Sci.*, *64*, 717–724.

Clarkson, D. T., M. Carvajal, T. Henzler, R. N. Waterhouse, A. J. Smyth, D. T. Cooke, and E. Steudle (2000), Root hydraulic conductance: Diurnal aquaporin expression and the effects of nutrient stress, *J. Exp. Bot.*, *51*, 61–70.

Collatz, G. J., M. Ribas-Carbo, and J. A. Berry (1992), Coupled photosynthesis-stomatal conductance model for leaves of c4 plants, *Aust. J. Plant Physiol.*, *19*, 519–538.

Cowan, I. R. (1977), Stomatal behaviour and environment, *Adv. Bot. Res.*, *4*, 117–228.

Cowan, I. R., and G. D. Farquhar (1977), Stomatal function in relation to leaf metabolism and environment, *Soc. Exp. Biol. Symp.*, *31*, 471–505.

Daly, E., A. Porporato, and I. Rodriguez-Iturbe (2004a), Coupled dynamics of photosynthesis, transpiration, and soil water balance. i. From hourly to daily time scale, *J. Hydrometeorol.*, *5*, 546–558.

Daly, E., A. Porporato, and I. Rodriguez-Iturbe (2004b), Coupled dynamics of photosynthesis, transpiration, and soil water balance. part ii: Stochastic analysis and ecohydrological significance, *J. Hydrometeorol.*, *5*, 559–566.

Damesin, C., S. Rambal, and R. Joffre (1998), Seasonal and annual changes in leaf $\delta^{13}C$ in two co-occurring mediterranean oaks: Relations to leaf growth and drought progression, *Funct. Ecol.*, *12*, 778–785.

Dixon, H., and J. Joly (1894), On the ascent of sap, *Phil. Trans. R. Soc. London, Ser. B*, *186*, 576.

Donovan, L. A., and J. R. Ehleringer (1994), Carbon isotope discrimination, water-use efficiency, growth, and mortality in a natural shrub population, *Oecologia*, *100*, 347–354.

Ehleringer, J. (1993), Variation in leaf carbon isotope discrimination in encelia farinosa: Implications for growth, competition, and drought survival, *Oecologia*, *95*, 340–346.

Farquhar, G. D., and S. C. Wong (1984), An empirical model of stomatal conductance, *Aust. J. Plant Physiol.*, *11*, 191–210.

Farquhar, G. D., S. von Caemmerer, and J. A. Berry (1980), A biochemical model of photosynthetic CO_2 assimilation in leaves of C_3 species, *Planta*, *149*, 78–90.

Field, C. (1983), Allocating leaf nitrogen for the maximization of carbon gain: Leaf age as a control on the allocation program, *Oecologia*, *56*, 341–347.

Field, C., and H. Mooney (1986), The photosynthesis-nitrogen relationship in wild plants, in *On the Economy of Plant Form and Function*, edited by T. J. Givnish, pp. 25–55, Cambridge Univ. Press, Cambridge, UK.

Franks, P. J., I. R. Cowan, and G. D. Farquhar (1998), A study of stomatal mechanisms using the cell pressure probe, *Plant, Cell Environ.*, *21*, 94–100.

Gimenez, C., V. J. Mitchell, and D. W. Lawlor (1992), Regulation of photosynthetic rate of two sunflower hybrids under water stress, *Plant Physiol.*, *98*, 516–524.

Gunasekera, D., and G. A. Berkowitz (1993), Use of transgenic plants with rubisco antisense DNA to evaluate the rate limitation of photosynthesis under water stress, *Plant Physiol.*, *103*, 629–635.

Hetherington, A. M., and F. T. Woodward (2003), The role of stomata in sensing and driving environmental change, *Nature*, *424*, 901–908.

Hirose, T., and M. J. A. Werger (1987), Maximizing daily canopy photosynthesis with respect to the leaf nitrogen allocation pattern in the canopy, *Oecologia*, *72*, 520–526.

Hubbard, R. M., M. G. Ryan, V. Stiller, and J. S. Sperry (2001), Stomatal conductance and photosynthesis vary linearly with plant hydraulic conductanc in Ponderosa Pine, *Plant Cell Environ.*, *24*, 113–121.

Huber, B. (1928), Weitere quantitative untersuchungen uber das wasserleitungssystem der pflanzen, *Jb Wiss. Bot*, *67*, 877–959.

Jones, H. G. (1998), Stomatal control of photosynthesis and transpiration, *J. Exp. Bot.*, *49*, 387–398.

Kabat, P. et al. (2004), *Vegetation, Humans and the Climate*, Springer, Berlin.

Katul, G., R. Leuning, and R. Oren (2003), Relationship between plant hydraulic and biochemical properties derived from a steady-state coupled water and carbon transport model, *Plant Cell Environ.*, *26*, 339–350.

Keck, R. W., and J. S. Boyer (1974), Chloroplast response to low leaf water potentials. iii. Differing inhibition of electron transport and photophosphorylation., *Plant Physiol.*, *53*, 474–479.

Kerkhoff, A. J., S. N. Martens, and B. T. Milne (2004), An ecological evaluation of Eagleson's optimality hypotheses, *Funct. Ecol.*, *18*, 404–413.

Khalil, A. A. M., and J. Grace (1992), Acclimation to drought in *Acer pseudoplantanus L.* (Sycamore) seedlings, *J. Exp. Bot.*, *43*, 1591–1602.

Korner, C., G. D. Farquhar, and S. C. Wong (1991), Carbon isotope discrimination by plants follows latitudinal and altitudinal trends, *Oecologia*, *88*, 30–40.

Kucharik, C. J., J. A. Foley, C. Delire, V. A. Fisher, M. T. Coe, J. D. Lenters, C. Young-Molling, N. Ramankutty, J. M. Norman, and S. T. Gower (2000), Testing the performance of a dynamic global ecosystem model: Water balance, carbon balance and vegetation structure, *Global Biogeochem. Cycles*, *14*, 795–825.

Laio, F., A. Porporato, L. Ridolfi, and I. Rodriguez-Iturbe (2001), Plants in water-controlled ecosystems: active role in hydrological processes and response to water stress ii. Probabilistic soil moisture dynamics, *Adv. Water Resour.*, *24*, 707–723.

Lloyd, J., and G. D. Farquhar (1994), ^{13}C discrimination during CO_2 assimilation by the terrestrial biosphere, *Oecologia*, *99*, 201–215.

Lloyd, J., and G. D. Farquhar (1996), The CO_2 dependence of photosynthesis, plant growth responses to elevated atmospheric CO_2 concentrations and their interaction with soil nutrient status. i. general principles and forest ecosystems, *Funct. Ecol.*, *10*, 4–32.

Magnani, F., M. Mencuccini, and J. Grace (2000), Age-related decline in stand productivity: The role of structural acclimation under hydraulic constraints, *Plant Cell Environ.*, *23*, 251–263.

Makela, A., F. Berninger, and P. Hari (1996), Optimal control of gas exchange during drought: Theoretical analysis, *Ann. Bot.*, *77*, 461–467.

Medrano, H., M. A. J. Parry, X. Socias, and D. W. Lawlor (1997), Long term water stress inactivates rubisco in subterranean clover, *Ann. Appl. Biol.*, *131*, 491–501.

Medrano, H., J. M. Escalona, J. Bota, J. Gulias, and J. Flexas (2002), Regulation of photosynthesis of C3 plants in response to progressive drought: Stomatal conductance as a reference parameter, *Ann. Bot.*, *89*, 895–905.

Meidner, H., and T. Mansfield (1968), *Physiology of Stomata*, Mc-Graw Hill, Maidenhead, UK.

Meinzer, F. C. (2002), Coordination of vapor and liquid phase water transport properties in plants, *Plant, Cell Environ.*, *25*, 265–274.

Meinzer, F. C., P. W. Rundel, G. Goldstein, and M. R. Sharifi (1992), Carbon isotope composition in relation to leaf gas exchange and environmental conditions in Hawaiian metrosideros polymorpha populations, *Oecologia*, *91*, 305–311.

Meinzer, F. C., M. J. Clearwater, and G. Goldstein (2001), Water transport in trees: Current perspectives, new insights and some controversies, *Environ. Exp. Bot.*, *45*, 239–262.

Mencuccini, M. (2003), The ecological significance of long-distance water transport: Short-term regulation, long-term acclimation and the

hydraulic costs of stature across plant life forms, *Plant, Cell Environ.*, *26*, 163–182.
Milly, P. C. D. (1991), A refinement of the combination equations for evaporation, *Surv. Geophys.*, *12*, 145–154.
Parsons, L. R., and P. J. Kramer (1974), Diurnal cycling in the root resitance to water flow, *Plant Physiol.*, *30*, 19–23.
Quick, W. P., M. M. Chaves, R. Wendler, M. David, M. L. Rodrigues, J. A. Passaharinho, J. S. Pereira, M. D. Adcock, R. C. Leegood, and M. Stitt (1992), The effect of water stress on photosynthetic carbon metabolism in four species grown under field conditions, *Plant Cell Environ.*, *22*, 25–35.
Reich, P. B., M. B. Walters, D. S. Ellsworth, J. M. Vose, J. C. Violin, C. Gresham, and W. D. Bowman (1998), Relationships of leaf dark respiration to leaf nitrogen, specific leaf area and leaf life-span: A test across biomes and functional groups, *Ecology*, *114*, 471–482.
Reich, P. B., D. S. Ellsworth, M. B. Walters, J. M. Vose, C. Gresham, J. C. Violin, and W. D. Bowman (1999), Generality of leaf trait relationships: A test across six biomes, *Ecology*, *80*, 1955–1969.
Rodriguez-Iturbe, I., A. Porporato, F. Laio, and L. Ridolfi (2001), Intensive or extensive use of soil moisture: Plant strategies to cope with stochastic water availability, *Geophys. Res. Lett.*, *28*, 4495–4497.
Ryan, M. G. (1991), Effects of climate change on plant respiration, *Ecol. Appl.*, *1*, 157–167.
Schimel, D. S. (1995), Terrestrial ecosystems and the carbon cycle, *Global Change Biology*, *134*, 77–91.
Schulze, E. D., J. Cermk, R. Matyssek, M. Penka, R. Zimmermann, F. Vasicek, W. Gries, and J. Kucera (1985), Canopy transpiration and water fluxes in the xylem of the trunk of larix and picea trees a comparison xylem flow, porometer and cuvette measurements, *Oecologia*, *66*, 475–483.
Sellers, P. J., D. A. Randall, G. J. Collatz, J. A. Berry, C. B. Field, D. A. Dazlich, C. Zhang, G. D. Collelo, and L. Bounou (1996), A revised land surface parameterization (SiB2) for atmospheric GCMS. part I: Model Formulation, *J. Clim.*, *9*, 676–705.
Sellers, P. J., et al. (1997), Modeling the exchanges of energy, water, and carbon between continents and the atmosphere, *Science*, *275*, 502–509.
Smith, T., and M. Huston (1989), A theory of the spatial and temporal dynamics of plant communities, *Vegetatio*, *83*, 49–69.
Smith, T. M., H. H. Shugart, and F. I. Woodward (1997), *Plant Functional Types: Their Relevance to Ecosystem Properties and Global Change*, Cambridge Univ. Press, Cambridge, UK.
Sparks, J. P., and J. R. Ehleringer (1997), Leaf carbon isotope discrimination and nitrogen content for riparian trees along elevational transects, *Oecologia*, *109*, 362–367.
Sperry, J. S., U. G. Hacke, R. Oren, and J. P. Comstock (2002), Water deficits and hydraulic limits to leaf water supply, *Plant, Cell Environ.*, *25*, 251–263.
Tezara, W., V. J. Mitchell, S. D. Driscoll, and D. W. Lawlor (1999), Water stress inhibits plant photosynthetisis by decreasing coupling factor and ATP, *Nature*, *401*, 914–917.
Thornley, J. H. M., and M. G. R. Cannell (2000), Modelling the components of plant respiration: Representation and realism, *Ann. Bot.*, *85*, 55–67.
Tuzet, A., A. Perrier, and R. Leuning (2003), A coupled model of stomatal conductance, photosynthesis and transpiration, *Plant Cell Environ.*, *26*, 1097–1116.
Van der Tol, C., A. J. Dolman, M. J. Waterloo, and K. Raspor (2007), Topography induced spatial variations in diurnal cycles of assimilation and latent heat of mediterranean forest, *Biogeosciences*, *4*, 137–154.
van der Tol, C., H. J. Dolman, M. J. Waterloo, and A. G. C. A. Meesters (2008), Optimum vegetation characteristics, assimilation and transpiration during a dry season: 2. Model evaluation, *Water Resour. Res.*, doi:10.1029/2007WR006243, in press.
Warren, C. R., and M. A. Adams (2006), Internal conductance does not scale with photosynthetic capacity: implications for carbon isotope discrimination and the economics of water and nitrogen use in photosynthesis, *Plant Cell Environ.*, *29*, 192–201.
Whitehead, D., N. J. Livingstone, F. M. Kelliher, K. P. Hogan, S. Pepin, T. M. McSeveny, and J. N. Byers (1996), Response of transpiration and photosynthesis to a transient change in illuminated foliage area for a *Pinus radiata* D Don tree, *Plant Cell Environ.*, *19*, 949–957.
Wilson, K. B., D. D. Baldocchi, and P. J. Hanson (2000), Spatial and seasonal variability of photosynthesis parameters and their relationship to leaf nitrogen in a deciduous forest, *Tree Physiol.*, *20*, 565–578.
Wong, S. C., I. R. Cowan, and G. D. Farquhar (1979), Stomatal conductance correlates with photosynthetic capacity, *Nature*, *282*, 424–426.
Younis, H. M., J. S. Boyer, and Govindjee (1979), Conformation and activity of chloroplast coupling factor exposed to low chemical potential of water in cells, *Biochem. Biophys. Acta*, *548*, 328–340.
Zhang, J., and W. J. Davies (1989), Abscisic acid produced in dehydrating roots may enable the plant to measure the water status of the soil, *Plant Cell Environ.*, *12*, 73–81.
Zhang, J., U. Schurr, and W. J. Davies (1987), Control of stomatal behaviour by abscisic acid which apparently originates in the roots, *J. Exp. Bot.*, *38*, 1174–1181.

A. J. Dolman, A. G. C. A. Meesters, and M. J. Waterloo, Department of Hydrology and Geo-Environmental Sciences, Vrije Universiteit Amsterdam, De Boelelaan 1085, 11081 HV Amsterdam, Netherlands.

C. van der Tol, ITC International Institute for Geo-Information Science and Earth Observation, P.O. Box 6, 7500 AA Enschede, Netherlands. (tol@itc.nl)